Nuclear Instruments and Methods in Physics Research A, Proc. CPO5 (1999)

High-accuracy field description of particle spectrographs

Ralf Degenhardt* and Martin Berz

Department of Physics and Astronomy and National Superconducting Cyclotron Laboratory, Michigan State University, MI 48824

For high-resolution spectrographs with large phase space acceptance the hardware correction of all the relevant aberrations requires so many multipole elements that software correction methods are often more adequate. In this case, the obligatory computation of the higher-order transfer map becomes feasible if the (three-dimensional) magnetic field within the spectrograph can be approximated with sufficient accuracy in an analytical form. For this purpose, we present an approach that allows the use of midplane measurements or alternatively measurements in several planes resulting in a global Maxwellian field that suppresses local measurement inaccuracies. It is based on a modified charge density method generating the magnetic field by a superposition of Gaussian charge distributions. The accuracy of the method is assessed through test cases for which analytical solutions of the field components are known. A maximum relative inaccuracy of the magnetic field in the midplane smaller than $\pm 10^{-4}$ is obtained in the relevant field area. In addition, we obtain a good agreement comparing the multipole content of the analytical field solution with the one of the approximated field.

1 Introduction

In the case of nuclear particle spectrographs with large aperture (solid angles $\geq 10msr$) and with high energy acceptance ($\geq 10\%$), the correction of all the relevant aberrations would require a large number of additional multipole elements in order to achieve an acceptable resolution. Therefore, methods based on the reconstruction of the trajectories in the particle spectrograph and the subsequent reconstructive correction of the aberrations seem to be a more appropriate alternative [1]. The S800 [2], which was recently commissioned at Michigan State University's National Superconducting Cyclotron Laboratory, is such a spectrograph designed for an energy resolution of one part in 10000. Because of its large phase space acceptance, aberrations of at least up to fifth order are assumed to be relevant and may impair the achievable resolution.

The software correction of aberrations requires the computation of the higher-order transfer map that relies on the precise knowledge of the (three-dimensional) magnetic field of the particle spectrograph. If the magnetic field, which is measured for this purpose, can be approximated with sufficient accuracy in an analytical form, one can take full advantage of differential algebraic (DA) methods [3, 4]. Using only field information in one plane, the midplane of the sector magnet, one directly notices the influence of the inaccuracies in the measurement, particularly when the higher-order derivatives of the approximated field are determined. This means that higher-order optical properties might be calculated less precisely, since derivatives of the midplane field of order n contribute to the nth-order aberrations. Therefore, we present an approach based on the charge density method that not only allows to use midplane measurements, but also to readily employ measurements taken in several additional planes. We estimate the accuracy that can be obtained by our algorithm by applying it to the approximation of a reference field that can be represented analytically.

2 An Analytical Reference Field

As reference field we consider the magnetic field of rectangular iron bars with inner surfaces ($y = \pm y_0$) parallel to the midplane ($y = 0$). The geometry of

* Present Address: ICT GmbH, Ammerthalstraße 20, D-85551 Heimstetten, Germany.

these uniformly magnetized bars, which are assumed to be infinitely extended in the $\pm y$-directions, is defined by:

$$-x_0 \le x \le +x_0, \;\; |y| \ge y_0, \;\; -z_0 \le z \le +z_0. \quad (1)$$

For this region of magnetization one obtains for the y-component of the magnetic bar field $H_y^B(x,y,z)$ an analytical solution of the form [5]:

$$H_y^B(x,y,z) = \hat{H}_0^B \sum_{i,j} (-)^{i+j} \cdot \left[\arctan\left(\frac{x_i \cdot z_j}{y_+ \cdot R_{ij}^+}\right) + \arctan\left(\frac{x_i \cdot z_j}{y_- \cdot R_{ij}^-}\right) \right] \quad (2)$$

with $i,j = 1,2$ and where the following abbreviations are introduced:

$$\begin{aligned} x_1 &= x - x_0 \quad , \quad x_2 = x + x_0, \\ y_- &= y_0 - y \quad , \quad y_+ = y_0 + y, \\ z_1 &= z - z_0 \quad , \quad z_2 = z + z_0, \end{aligned}$$

and

$$R_{ij}^{\pm} = (x_i^2 + y_\pm^2 + z_j^2)^{1/2}.$$

$\hat{H}_0^B$ determines the maximum of this field component which is taken at the bars.

From $H_y^B(x,y,z)$ we generate reference field points on a regular grid in the midplane (see Fig. 1) as well as in planes above and below the midplane as indicated in Fig. 2.

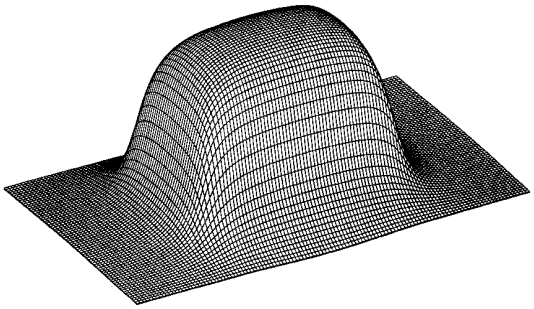

Figure 1: Analytical reference field $H_y^B(x,0,z)$. We have chosen here the geometry: $x_0 = 2.5D$, $z_0 = 3.75D$ and $y_0 = D/2$ in units of the gap distance D between the two bars.

3 The Modified Charge Density Method

In order to benchmark the performance of our method, we approximate in the following the field data obtained from the reference field, described in section 2, in the same way as measurement data can be approximated. For this purpose, image charges are placed on regular grids parallel to the midplane (see Fig. 2). Using the charge density method [6] in the magnetostatic case, one can not assume in the general case that the scalar potential is constant on the boundary of the magnets. Therefore, we determine the strengths of the individual charges by a least-square fit of the field values at the reference points. In addition, we choose the planes on which the image charges are placed not to coincide with the horizontal surfaces of the iron bars.

In order to reduce any fine structure due to the influence of individual image charges, we use extended distributions in the form of three-dimensional Gaussian charge distributions [7]:

$$\rho(r) = \rho_0 \cdot e^{-(r/a)^2}, \quad (3)$$

where a is a measure for the width of the Gaussian, and ρ_0 determines the strength of the individual image charge. A magnetic field generated by a superposition of Gaussian charge distributions automatically satisfies Maxwell's equations.

The ith Gaussian positioned at the point (x_i, y_i, z_i) makes a contribution to the y-component of the magnetic field of the form:

$$H_{y,i}^C(x,y,z) = (y - y_i)/r_i^3 \cdot \rho_i \cdot \left[-\frac{a_i^2}{2} r_i \, e^{-(r_i/a_i)^2} + \frac{\sqrt{\pi}}{4} a_i^3 \, \mathrm{erf}\left(\frac{r_i}{a_i}\right) \right], \quad (4)$$

where $r_i = [(x-x_i)^2 + (y-y_i)^2 + (z-z_i)^2]^{1/2}$ and $\mathrm{erf}(u) = 2/\sqrt{\pi} \int_0^u e^{-u'^2} du'$ is the error function. The total field $H_y^C(x,y,z)$ is obtained by summing over all individual Gaussians. Adjusting their width appropriately, the superposition of regularly distributed Gaussians has proven to result in a rather smooth global field distribution.

One of the grids with Gaussian charge distributions is located in the present configuration at $y = \pm D$ and is larger than the cross-section of the bars (see Fig. 2). The distance between the Gaussians is chosen to be approximately a. A second grid with $a = 1.5D$ (not

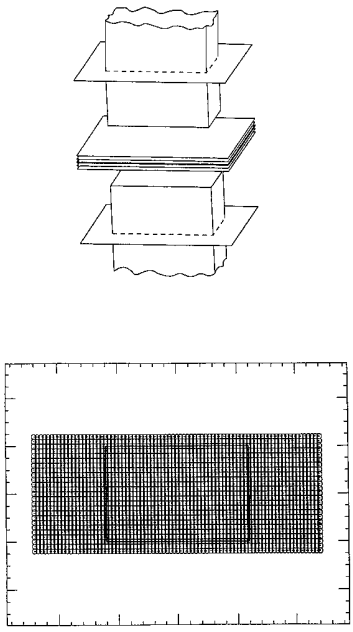

Figure 2: Schematic arrangement of the rectangular iron bars indicating in the gap the planes that contain the reference field data and two planes on which image charges are placed. Bottom: Grid generated by Gaussian charge distributions. The bold inner rectangle indicates the cross-section of the bars. Note the smaller step-size in the horizontal direction in order to describe the fall-off of the fringe field in more detail.

depicted in Fig. 2) is placed at the planes $y = \pm 5D$, so that eight Gaussians cover almost the entire area shown in Fig. 2. Since the Gaussian distribution is approximately zero at a distance of $3a$, it is assumed that $\rho = 0$ at the reference planes, which are located at $y = 0, \pm 0.125D$, and $\pm 0.25D$. For the computations we make also use of the midplane symmetry of the magnet.

The least-square algorithm results in a quadratic matrix which has to be inverted in order to determine the strengths of the individual charges. In total, we placed $N_C = 535$ Gaussians on a quarter of the whole arrangement, taking advantage of the geometrical symmetry of the bars. The dimension of the matrix is given by the number of image charges and their strengths are determined in the present case by $N_R = 10125$ reference field points.

4 Computational Results

We concentrate in the following on the calculation of the difference between the reference field and its approximation on a strip through the magnet in order to assess the applicability of our method to the description of sector magnets. In this case, our main focus is the proper representation of the entrance and exit fringe field region of the magnet. The strip covers 75% of the width of the bars and is twice as long as the bars. In this area, considered as relevant, the maximum difference between the y-component of the two fields in the midplane $\Delta H_y(x,0,z) = H_y^C(x,0,z) - H_y^B(x,0,z)$ normalised on $H_y^B(0,0,0)$ is smaller than 10^{-4} (see Fig. 3, top). The maximum differences occur in a rather limited region of the fringe-field. The average error over the entire strip is estimated to be one order of magnitude smaller.

When experimentally obtained magnetic fields have to be approximated, local measurement errors are superimposed on the actual field data. In order to simulate the noise on measured field data, we add/subtract on every point of the reference field a field difference ΔH^N, which is randomly distributed in an interval $\pm \Delta H^N_{max}$. In the case $\Delta H^N_{max}/H_y^B(0,0,0) = 10^{-4}$, the precision with which we can approximate the reference field is essentially unchanged. Overall, the average approximation error increases slightly due to the noise. Nevertheless, as long as the amplitude of the "noise" is within the range of the precision of the charge density method, this kind of "noise" does not negatively affect the accuracy of the field approximation.

When the "noise" amplitude is increased by a factor of five, we find the expected beneficial result that the method provides smoothing of this "noisy" data. In this case the relative field difference $\Delta H_y(x,0,z)/H_y^B(0,0,0)$ is smaller than $1.5 \cdot 10^{-4}$. The areas of maximal field differences are not restricted to the fringe field region anymore, resulting in a difference pattern that is dominated by the "noise".

4.1 Multipole Content

In order to calculate the multipole content of the analytical reference field and the one determined by the charge density method, we perform an expansion of

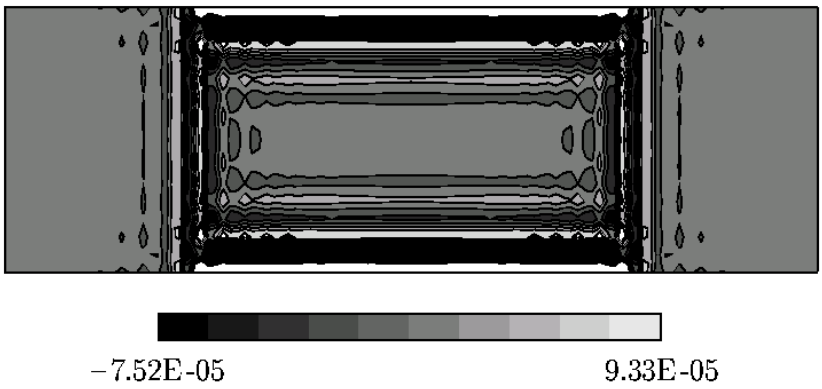

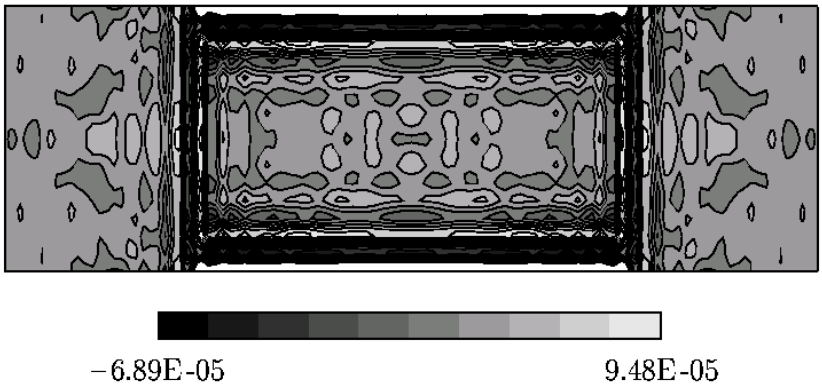

Figure 3: Normalised field difference $(H_y^C(x,0,z) - H_y^B(x,0,y))/H_y^B(0,0,0)$ on a strip through the bar covering 75% of its total width. Top: No "noise" is added to the reference field. Middle: With "noise" of amplitude $\Delta H_{max}^N/H_y^B(0,0,0) = 1{\cdot}10^{-4}$. Bottom: With "noise" of amplitude $\Delta H_{max}^N/H_y^B(0,0,0) = 5{\cdot}10^{-4}$.

the magnetic scalar potential

$$\psi(x,y,z) = \sum_{k=0}^{n}\sum_{l=0}^{n} a_{kl}(z)\, x^k y^l. \qquad (5)$$

In the case of midplane symmetry ($a_{k0} = 0$), the multipole coefficients a_{kl} with $l \geq 2$ are uniquely determined by the coefficients a_{k1}.

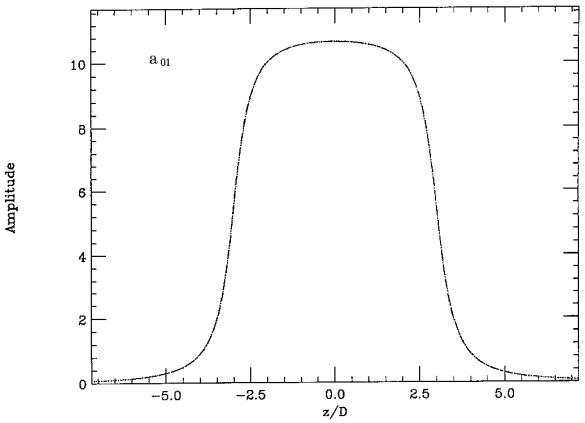

Figure 4: Multipole coefficient a_{01} along the z-axis through the magnet for the analytical reference field and its approximation by the charge density method.

If the components of the fields or the magnetic scalar potential in the midplane are known in an analytical form, the decomposition into the individual multipole moments can immediately be calculated within a DA-based framework [4]. For particle optics calculations up to fifth order, the relevant coefficients are $a_{01}(z), a_{21}(z)$, and $a_{41}(z)$. The coefficient $a_{01}(z)$ describes the field distribution while $a_{21}(z)$ and $a_{41}(z)$ determine the second and fourth derivative with respect to x. In the case of the bar field, derivatives in x-direction seem to be more sensitive than for a homogenous sector magnet. Therefore, we assume that the accuracy which we obtain for the analytical reference field is a reasonable estimate for the accuracy that we can expect in the case of homogeneous sector magnets including higher-order derivatives.

Using the code COSY INFINITY [4], we calculated the distribution of the coefficients $a_{01}(z), a_{21}(z)$, and $a_{41}(z)$ for the bar field and its approximated field. The results are shown in Fig. 4-6. As one can see, the second derivatives agree very well while a slight deviation is noticeable for the fourth derivative.

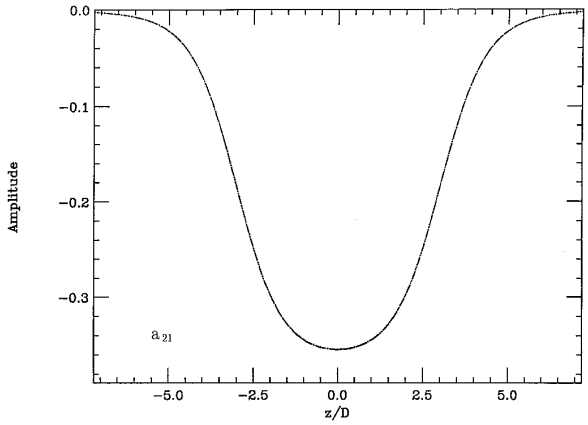

Figure 5: Multipole coefficient $a_{21(z)}$ as in Fig. 4.

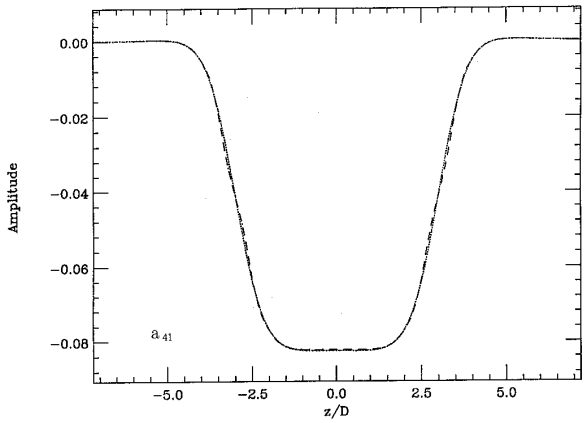

Figure 6: Multipole coefficient $a_{41(z)}$ as in Fig. 4.

5 Conclusion

One of the limiting factors for the obtainable accuracy in the approximation of measured magnetic dipole fields can be the noise on the available data. Although in such a case the noise may not have an essential influence on the y-component of the field in the midplane, its effect on the derivatives might not be negligible. Therefore, an additional smoothing of measured field data seems advisable as soon as higher-order optics computations have to be performed [8]. Nevertheless, since the modified image charge method presented here has proven to compensate for noise up to a certain extent, the importance of the actual smoothening algorithm should be less

critical.

Acknowledgement

This work was supported by the U.S. National Science Foundation under contract No. PHY 89-13815 and the Alfred P. Sloan Foundation. We thank G.H. Hoffstätter for several fruitful discussions on this subject.

References

[1] M. Berz, K. Joh, J.A. Nolen, B.M. Sherill, and A.F. Zeller, Phys. Rev. C 47 (1993) 537.

[2] J.A. Nolen, A.F. Zeller, B.M. Sherill, J.C. DeKamp, and J. Yurkon, Technical Report MSUCL-694, National Superconducting Cyclotron Laboratory, Michigan State University, East Lansing, MI 48824, USA, (1989).

[3] M. Berz, AIP Conference Proccedings 249 (1991) 456.

[4] K. Makino and M. Berz, COSY INFINITY Version 8, these Proceedings.

[5] M.M. Gordon and T. Taivassalo, Nucl. Instrum. and Methods Phys. Res. A247 (1986) 423.

[6] T. Mulvey and M.J. Wallington, Rep. Prog. Phys. 36 (1973) 347.

[7] M. Berz, IEEE Trans. Electron Devices 35 (1988) 2002.

[8] K. Makino, PhD thesis, Michigan State University, East Lansing, MI 48824, USA, 1989.